FORCED CONVECTION THERMAL BOUNDARY LAYER DEVELOPMENT IN A POROUS MEDIA NEAR A WALL WITH VARIABLE TEMPERATURE BOUNDARY CONDITION

Mrs. Luma F. Ali
Mech. Engr. Dept.
College of Engr.
University of Baghdad
Baghdad-Iraq

ABSTRACT

The behavior of forced convection heat transfer characteristics through and over porous layer near a heated flat plate at variable temperature has been investigated numerically. Two cases of variable wall temperature boundary condition are studied. The first case is of linear temperature variation with position along the flat plate and the second case is of sinusoidal temperature variation with time of heating. The flow field in the porous region is governed by the Darcy-Brinkman-Forchheimer equation, the thermal field in the porous region by the energy equation and the part over the porous matrix includes flow and heat transfer equations. Solutions of the problem have been carried out using a finite difference method through the use of a stream function-vorticity transformation. The effects of various governing dimensionless parameters, Darcy number, Reynolds number, Prandtle number as well as the inertia parameter are thoroughly explored. The variation of the non-dimensional period and amplitude values of the sinusoidal temperature distinction with time was also studied. Good results were obtained and reported graphically. It was found that the local Nusselt number on the flat plate increases with the increasing of the increasing non-dimensional values of period and amplitude individually.

الخلاصة:

يتناول البحث دراسة خصائص انتقال الحرارة بالحمل القسري خلال و فوق طبقة وسط مسامي موضوعة فوف صفيحة ذات درجة حرارة متغيرة باستخدام الطريقة العددية للفروقات المحددة. لقد تضمنت الدراسة حالتان من تغير درجة الحرارة كشرط حدي للجزء السفلي من الطبقة المسامية. ان الحالة الاولى كانت لتغير درجات الحرارة خطيا مع البعد على طول الصفيحة. اما الحالة الثانية فان التغير كان بشكل موجي مع الزمن. تضمن النموذج الرياضي للجريان خلال الوسط المسامي معادلة الجريان بالاعتماد على صياغة (Brinkman-Forchheimer) المستمدة من قانون دارسي و معادلة الطاقة خلال الوسط المسامي و الجزء الاخر للجريان فوق الوسط المسامي. تم حل المعادلات الحاكمة عدديا بأستخدام طريقة الفروق المحددة. و قد استخدمت طريقة (الدوامية-دالة الانسياب). خلال البحث تم دراسة تأثير عدد من المجاميع اللابعدية مثل رقم دارسي، رقم رينولدز، رقم برانتل كذلك تأثير القصور الذاتي. بالاضافة الى ذلك تم دراسة تأثير التغير في طول و ارتفاع الموجة اللابعدية لتغير درجة الحرارة الموجي مع الزمن. لقد ذُكِرتْ النتائج بشكل تخطيطي و تم الحصول على النَتائِج الجيدة. و قد وُجِدَ من هذه النتائج إن رفم نسلت الموضعي على طول الصفيحة يزداد بزيادة طول و ارتفاع الموجة اللابعدية كل على حدة.

KEYWORDS: Porous Media, Forced Convection, Heat Transfer, Numerical Solution.

INTRODUCTION

Forced convection heat transfer through porous media has a major topic for various studies during the past decades due to many engineering applications such as thermal insulation engineering, water movements in geothermal reservoirs, underground spreading of chemical waste, thermal insulation, direct-contact heat exchangers, nuclear waste repository, grain storage, and enhanced recovery of petroleum reservoir. The heat transfer with forced convection in porous media is an interesting and challenging physical problem; therefore a considerable attention was given to this type of problems by accomplishing theoretical and experimental studies.

The problem of forced convection flow and heat transfer along a flat plate in a porous medium was examined by Beckermann & Viskanta [1987] including both, the inertia and boundary effects, while porosity variations close to the wall are not considered. They derived the velocity and temperature profiles for the fully-developed momentum boundary layer and from the results they determined the wall shear stress and the Nusselt number as functions of modified Reynolds and Prandtle numbers. In addition, Vafai and Thiyagaraja [1987] analytically studied the fluid flow and heat transfer for three types of interfaces, namely, the interface between two different porous media, the interface separating a porous medium from a fluid region and the interface between a porous medium and an impermeable medium. Another related problem is that of Poulikakos and Kazmierczak [1987]. In that work a fully developed forced convection in a channel filled with a porous matrix was investigated and the existence of a critical thickness of the porous layer at which the value of Nusselt number reaches a minimum was demonstrated.

A fundamental investigation on the effects of employing intermittently porous cavities for regulating and modifying the flow and temperature fields was done by Vafai & Huang [1994]. They used a general flow model that accounts for the effects of the impermeable boundary and inertial effects to describe the flow inside the porous region and the solution of the problem has been carried out using finite difference method through the use of a stream function-vorticity transformation. Also the effects of various governing dimensionless parameters, such as the Darcy number, Reynolds number, Prandtle number and the inertia parameter were thoroughly explored. Then Huang & Vafai [1994] presented an analytical solution for forced convection boundary layer flow and heat transfer through a composite porous/fluid system by considering a layer of porous media over a flat plat with constant temperature boundary condition. The details of the interaction phenomena occurring in the porous medium and the fluid layer were systematically analyzed, revealing the effects of various parameters governing the physics of the problem. Their results presented a comprehensive yet easy comparative base for numerical solutions addressing this type of interfacial transport and their analysis provided a rather accurate simulation of the interfacial transport.

Furthermore a finite-volume computational model had been developed by Vadakkan [2001] to analyze the steady performance of a pin fin array experiencing forced convection in a duct. This pin fin array was considered using transport equations of porous media. The analysis had been done utilizing two different approaches in solving the temperature fields in the porous structure and indicated that there is a significant difference between the solid and fluid temperature at higher values of porosity and lower values of the interstitial heat transfer coefficient.

For an unsteady forced convection on a flat plate embedded in the fluid-saturated porous medium with inertia effect and thermal dispersion, Cheng & Lin [2002] presented a precise and rigorous method to obtain the entire solution from one-dimensional transient conduction to steady forced convection in porous medium under conditions of uniform wall temperature and uniform heat flux, respectively. In addition, the aim of their work is to quantify the effect of inertia force on the intermediate regime of unsteady forced convection in a porous medium. Huang et al. [2005] carried out a numerical study for enhanced heat transfer from multiple heated blocks in a channel by porous covers. The flow field was governed by the Navier-Stokes equation in the fluid region, the Darcy-Brinkman-Forchheimer equation in the porous region, and the thermal field by the energy equation. Solution of the coupled governing equations was obtained

using a stream function-vorticity analysis. This study details the effects of variations in the Darcy number, Reynolds number, inertial parameter, and two pertinent geometric parameters, to illustrate important fundamental and practical results.

In order to study the development of the forced convection thermal boundary layer in a definite layer of porous media near a wall with two types of temperature boundary condition, a flat plate of specified length and covered with definite height of porous media and a fluid with ambient velocity and temperature flowing over and through the porous matrix is taken into account in the present paper. Two cases for the lower boundary temperature condition are used; one is linear temperature variation with the length of the plate and the other is the temperature boundary condition that varies sinusoidally with time.

MATHEMATICAL FORMULATION

The configuration of the problem under investigation is depicted in **Fig. 1.** It includes a flat plate of length L covered with a porous media layer of height H . A fluid with constant temperature T_∞ and velocity u_∞ is flowing through and over this porous medium layer. In this study, it is assumed that the flow is laminar, incompressible, and two dimensional. In addition, the thermo-physical properties of the fluid and the porous matrix are assumed to be constant and the fluid-saturated porous medium is considered homogenous and isotropic and in local thermodynamic equilibrium with the fluid. For the fluid region the conservation equations for mass, momentum, and energy are [Vafai & Huang 1994]:

$$\frac{\partial \rho_f}{\partial t}+\nabla V_f=0 \qquad (1)$$

$$\frac{\partial V_f}{\partial t}+V_f.\nabla V_f=-\frac{1}{\rho_f}\nabla P_f+\upsilon_f\nabla^2.V_f \qquad (2)$$

$$\frac{\partial T_f}{\partial t}+V_f.\nabla T_f=\alpha_f\ \nabla^2 T_f \qquad (3)$$

Based on the Brinkman-Forchheimer-extended Darcy model, which accounts for the effects of the inertial and impermeable boundary, the mass, momentum and energy equations in the porous matrix can be expressed as [Vafai & Huang 1994]:

$$\varepsilon\frac{\partial \rho_f}{\partial t}+\rho_f.\nabla V_p=0 \qquad (4)$$

$$\frac{\rho_f}{\varepsilon^2}\left(\varepsilon\frac{\partial V_p}{\partial t}+V_p.\nabla V_p\right)=-\frac{1}{\rho_f}\nabla P_f - \left(\frac{\mu_{eff}}{K}+\frac{F.\varepsilon}{\sqrt{K}}\ V_m\right)V_P+\frac{\mu_{eff}}{\varepsilon}\nabla^2 V_p \qquad (5)$$

$$(\rho C)_f\left(\sigma\frac{\partial T_p}{\partial t}+V_p.\nabla T_p\right)=k_{eff}\nabla^2 T_p \qquad (6)$$

In order to express the governing equations in dimensionless form, the following non-dimensional quantities may be defined:

$$Y=\frac{y}{L},\ X=\frac{x}{L},\ V=\frac{v}{u_\infty},\ U=\frac{u}{u_\infty},\ P=\frac{p}{\rho u_\infty^2},$$
$$\theta=\frac{T-T_\infty}{T_W-T_\infty},\ V_m=\sqrt{\frac{u^2+v^2}{u_\infty^2}}=\sqrt{U^2+V^2},$$
$$\mathrm{Re}_L=\frac{\rho u_\infty L}{\mu},\ Da_L=\frac{K}{L^2},\ \mathrm{Pr}_f=\frac{\mu_f.Cp}{k_f},$$
$$\mathrm{Pr}_{eff}=\frac{\mu_f.Cp}{k_{eff}},\ \sigma=\frac{\varepsilon\rho_f\ Cp_f+(1-\varepsilon)\rho_s C_s}{\rho_f Cp_f},$$
$$t^*=\frac{tu_\infty}{L},\ AL=\frac{FL\varepsilon}{\sqrt{K}} \qquad (7)$$

After utilizing the above dimensionless groups and canceling the pressure term P from the resulted equations [Qahtan 2005], the vorticity and temperature equations respectively for the fluid region may be expressed as follows:

$$\frac{\partial \omega_f}{\partial t^*}+\frac{\partial (U\omega)_f}{\partial X}+\frac{\partial (V\omega)_f}{\partial Y}=\frac{1}{\mathrm{Re}_L}\left(\frac{\partial^2\omega_f}{\partial X^2}+\frac{\partial^2\omega_f}{\partial Y^2}\right) \qquad (8)$$

$$\frac{\partial \theta_f}{\partial t^*}+\frac{\partial (U\theta)_f}{\partial X}+\frac{\partial (V\theta)_f}{\partial Y}=\frac{1}{\mathrm{Re}_L\ \mathrm{Pr}_f}\left(\frac{\partial^2\theta_f}{\partial X^2}+\frac{\partial^2\theta_f}{\partial Y^2}\right) \qquad (9)$$

Whereas the vorticity and temperature equations for the porous region may be stated as the following two equations [Qahtan 2005]:

$$\varepsilon*\frac{\partial \omega_p}{\partial t^*}+\frac{\partial (U\omega)_p}{\partial X}+\frac{\partial (V\omega)_p}{\partial Y}=-\frac{\varepsilon^2}{\mathrm{Re}_L\,Da_L}\omega_p - AL.\varepsilon.V_m\omega_p-AL.\varepsilon\left(V_p\frac{\partial V_m}{\partial X}-U_p\frac{\partial V_m}{\partial Y}\right)+\frac{\varepsilon}{\mathrm{Re}_L}\left(\frac{\partial^2\omega_p}{\partial X^2}+\frac{\partial^2\omega_p}{\partial Y^2}\right) \qquad (10)$$

$$\sigma\frac{\partial\theta_p}{\partial t^*}+\frac{\partial(U\theta)_p}{\partial X}+\frac{\partial(V\theta)_p}{\partial Y}=\frac{1}{\mathrm{Re}_L\,\mathrm{Pr}_{eff}}\left(\frac{\partial^2\theta_p}{\partial X^2}+\frac{\partial^2\theta_p}{\partial Y^2}\right) \quad (11)$$

The governing equations above are cast in terms of the vorticity-stream formulation. Therefore the stream function and vorticity may be introduced as:

$$U=\frac{\partial\psi}{\partial Y},\ V=-\frac{\partial\psi}{\partial X} \quad (12)$$

$$\omega=\frac{\partial V}{\partial X}-\frac{\partial U}{\partial Y} \quad (13)$$

Where (ω) is the vorticity component perpendicular to the flow surface. Also the vorticity may be related to the stream function by using the stream function equation which may be formulated as:

$$-\omega=\frac{\partial^2\psi}{\partial X^2}+\frac{\partial^2\psi}{\partial Y^2}=\nabla^2\psi \quad (14)$$

The applicable boundary conditions necessary to complete the problem formulation are:

$$\left.\begin{array}{lll} X=0 & Y & \vartheta=0,U=1,V=0,\psi=Y,\omega=-\frac{\partial^2\psi}{\partial X^2} \\ X=1 & Y & \frac{\partial\vartheta}{\partial X}=\frac{\partial\omega}{\partial X}=\frac{\partial\psi}{\partial X}=\frac{\partial U}{\partial X}=\frac{\partial V}{\partial X}=0 \\ Y=0 & 0<X<1 & U=V=\psi=0,\omega=-\frac{\partial^2\psi}{\partial Y^2} \\ Y\to\infty & 0<X<1 & \vartheta=0,U=\frac{\partial\psi}{\partial Y}=1,\omega=-\frac{\partial^2\psi}{\partial X^2} \end{array}\right\} \quad (15)$$

In the present work two cases of boundary conditions where taken for the temperature condition at the lower boundary $Y=0$. The first case is taken as temperature boundary condition which varies linearly with X and it is expressed in non-dimensional form as:

$$\vartheta=X \quad (16)$$

While the second case for the lower boundary condition is the temperature that varies sinusoidally with time and formulated in non-dimensional form as follow:

$$\vartheta=1+a\sin\left(\frac{2\pi t^*}{\eta}\right) \quad (17)$$

In addition to the above boundary conditions, the two sets of conservation equations are coupled by the following matching conditions at the porous/fluid interface [Vafai & Huang 1994], [Huang & Vafai 1994]:

$$\left.\begin{array}{l} u\big|_{y=H^-}=u\big|_{y=H^+},v\big|_{y=H^-}=v\big|_{y=H^+} \\ p\big|_{y=H^-}=p\big|_{y=H^+},\mu_{eff}\frac{\partial v}{\partial y}\big|_{y=H^-}=\mu_f\frac{\partial v}{\partial y}\big|_{y=H^+} \\ \mu_{eff}\left(\frac{\partial u}{\partial y}+\frac{\partial v}{\partial x}\right)\Big|_{y=H^-}=\mu_f\left(\frac{\partial u}{\partial y}+\frac{\partial v}{\partial x}\right)\Big|_{y=H^+} \\ T\big|_{y=H^-}=T\big|_{y=H^+},k_{eff}\frac{\partial T}{\partial y}\big|_{y=H^-}=k_f\frac{\partial T}{\partial y}\big|_{y=H^+} \end{array}\right\} \quad (18)$$

and the initial conditions are:

$$\theta=\psi=\omega=0 \qquad \text{for} \qquad t^*=0 \quad (19)$$

In the present work, an explicit finite difference numerical technique is used in order to solve the flow and heat equations. The finite difference form of the fluid and porous media regions and boundary and initial conditions are formulated in the next section.

NUMERICAL SOLUTION

To solve the above partial differential equations, a finite difference numerical technique is employed. A grid of points is first established throughout the calculation domain. However, the uniform rectangular grid system is the same for the fluid and porous media regions.

An explicit finite difference method is utilized for the energy and vorticity equations (equations (8-11)) as recommended by [(Anderson et al. 1984) and (Fletcher 1987)]. In the explicit method, the vorticity and temperature are calculated at future time $(t^*+\Delta t^*)$ for any internal grid by using the vorticity and temperature values at time (t^*) for the specified grid and the neighbor grids which are known from the initial conditions of the problem under consideration. By employing this time matching technique the values of the vorticity and temperature for the whole domain will be known for each time step until reaching the steady state condition. This condition is attained when the value of the average Nusselt number for two consecutive runs would become less than 10^{-8}.

On the other hand, after formulating the stream function equation (equation (14)) in finite difference form, the relaxation method is utilized in order to solve the resulted algebraic equations iteratively at each time step by employing Gauss-Seidel iterative technique. In this method, convergence has been achieved when the absolute value of relative error for the whole grid points between two successive iterations, found by trial and error, was equal to 10^{-4}.

A computer program written in FORTRAN was used. Once the above algebraic flow and heat transfer equations is solved, the temperature distribution for internal and boundary grid points is identified. Then, when the steady state condition for the linear variation temperature boundary condition is reached and specified time for the sinusoidal variation with time temperature boundary condition is spend, the local Nusselt number value is found by employing the following formula [Anderson et al. 1984]:

$$Nu_X = -X * \frac{k_{eff}}{k_f} * \frac{-3\theta(i,1)+4\theta(i,2)-\theta(i,3)}{2\Delta Y} \qquad (20)$$

where k_{eff}/k_f is taken equal to one.

While the average Nusselt number is found by integrating the local Nusselt number along the plate length by employing the Simpson numerical integration rule as given in the following expression:

$$\overline{Nu} = \frac{1}{L}\int_0^L Nu_X \, dx \qquad (21)$$

RESULTS AND DISCUSSION

In the present paper, the numerical values for the case under consideration was taken for a porous media layer of height $H/L = 0.02$ and porosity equal to 0.92. The metal foams was used as a porous medium and the material was Aluminum $(606-T6)$ with thermal conductivity of $200\,W/m.K$. Two cases of the temperature boundary condition at the lower boundary of the porous matrix are studied. The first case is the linear temperature variation with position until reaching steady state condition and the second case is the sinusoidal temperature variation with time for a specified period of time. Several values of dimensionless parameters were taken in order to study their effects on the heat transfer behavior. The Reynolds number values were verified within the laminar and transition regions $(1*10^5 - 5*10^5)$, the Prandtle number values were taken for three most utilized fluids (air 0.7, water 7, and engine oil 100), three Darcy number values were considered $(8\times10^{-6},\ 2\times10^{-6},$ and $9\times10^{-7})$, and the effect of three inertial parameter values $(0.001076, 0.0025, 0.00323)$ were studied. Finally, the variation effect of the non-dimensional values of the sinusoidal temperature variation with time boundary condition was also investigated. These constant values were the non-dimensional amplitude a $(0.2,\ 0.4,$ and $0.8)$ and the non-dimensional period η $(0.005, 0.01,$ and $0.02)$.

A testing for the optimum distance between grid points in X direction was done and the relation between the average Nusselt number and the number of grid points was sketched in **Fig. 2** for the linear temperature variation with position and sinusoidal temperature variation with time cases. From this figure, it is shown that a 75 grid point in X direction is suitable to choose for the present case study. As well, similar test was made for the number of grid points in Y direction and it was found that the 75 grid point is appropriate.

The propagation of the temperature through and over the porous media for five instances is demonstrated in **Fig. 3** for the linear temperature variation case and in **Fig. 4** for the sinusoidal temperature variation case. It is clear from these figures that the temperature values through the porous matrix are high in the beginning because of the small thermal boundary layer effect. But after a period of time this layer is grown up and then the temperature decreases.

Effect of the Reynolds Number

The variation of the average Nusselt number versus time for three values of Reynolds number for linear temperature variation case is presented in **Fig. 5**. It is clear from this figure that the time required to reach steady state condition decreases with increasing Reynolds number values. The increasing of Reynolds number causes a bigger value of the inertia force with respect to the viscosity force and then increasing in the velocity gradient followed by decreasing of the

time required for steady state condition. The same behavior was obtained for the sinusoidal case for specific non-dimensional time (equal to two) as illustrated in **Fig. 6**. In this figure, only one value of Reynolds number is drawn because, in the sinusoidal temperature case, there is not any significant effect of Reynolds number variation on the average Nusselt number.

By referring to **Fig. 7** and **Fig. 8** it can be observed that the temperature gradient increases with the increasing of the Reynolds number. As a result, this increase in temperature gradient causes an increase in the local Nusselt number value as exposed in **Fig. 9** and **Fig. 10** for the linear and sinusoidal temperature variation respectively. Furthermore, the effect of the Reynolds number on the thermal boundary layer thickness for the two cases under study can be noticed from **Fig. 11** and **Fig. 12**. From these two figures, it can be deduced that the thermal boundary layer is grown inside the porous matrix only because of the solid structure of the porous media which causes a loss in the heat energy. As well, from these two figures it can be noticed that the thermal boundary layer thickness decreases with the Reynolds number increasing. This decreasing of the layer thickness is due to the sharp decreasing in the temperature gradient in the Y-direction because of the diffusion term small value.

Effect of the Darcy Number

Results for the effect of Darcy number variation are presented in several figures. In **Fig. 13** the relation between the average Nusselt number versus time for the linear temperature variation case is sketched. From this figure, it is clear that the time required for steady state condition decreases with the decreasing of the Darcy number values. This behavior is due to the increasing of the velocity gradient in Y-direction with the Darcy number decreasing values. Moreover, the decrease in Darcy number value means an increase in the flow uniformity and reduces vorticity and this leads to the reduction in the time required for steady state condition. Similar figure is presented for the sinusoidal temperature variation case for specific non-dimensional time value in **Fig. 14**. There is no significant change in Nusselt number values when the Darcy number is varied therefore only two cases were sketched in this figure.

The effect of Darcy number variation on the local Nusselt number along the flat plate is presented in **Fig. 15** and **Fig. 16**. From these figures, it is clear that the local Nusselt number increases with the decreasing of the Darcy number. This decrease in Darcy number with constant porosity cause a decreasing in the solid fraction volume and increasing in the heat transfer exposed area. As a result, a rising in the temperature slop in Y-direction is occurred as shown in **Fig. 17** and **Fig. 18** and consequently an increasing in the local and average Nusselt number values. **Fig. 19** and **Fig. 20** is adapted to the non-dimensional temperature distribution and the thermal boundary layer thickness. These two figures show that any reduction in Darcy number yields a decreasing in the thermal boundary thickness because of the enlarging in the velocity slop in Y-direction.

Inertial Effects

In order to study the inertia effect several figures are sketched. In **Fig. 21**, the relation between the average Nusselt number with time is illustrated. From this figure, it is clear that the time required to reach steady state condition decreases with the inertia effect increase. This behavior is due to the increasing in the velocity slop with inertia effect rising and then leads to a reduction in the time required for steady state condition. Similar figure is presented for the sinusoidal temperature variation but for specific value of time in **Fig. 22**. In addition, it can be noticed that the inertia is less effective than the Darcy number on the required time for steady state and this is because of the velocity slop value.

In **Fig. 23** and **Fig. 24**, the inertia effect on the local Nusselt number along the flat plate is illustrated for the linear and sinusoidal temperature variation. From these two figures it is shown that any increase in the inertia effect leads to a small reduction in local Nusselt number. This behavior is because of the small reduction in the temperature slope in Y-direction, as shown in **Fig. 25** and **Fig. 26**, and this slope reduction causes a small decreasing in the local and Average Nusselt number values. For the same reason, the thermal boundary layer thickness decreases with the inertia effect rising as depicted in **Fig. 27** and **Fig. 28**.

Effect of the Prandtle Number

To study the effects of the Prandtl number on the flow and temperature fields, three different Prandtle numbers were chosen such that they will cover a wide range of thermo-physical fluid properties such as the kinematics viscosity. The variation of the average Nusselt number versus time is shown in **Fig. 29** for linear temperature variation. From this figure, it is clear that whenever the kinematics viscosity is lower, the time required for steady state condition is higher. The reason of this trend is that, at specific Reynolds number, lower value of viscosity leads to smaller viscosity force and then smaller inertia and this needs more time to reach steady state. On the other hand, **Fig. 30** is sketched for the sinusoidal temperature variation and for specific time. It can be seen that the time required to reach a complete periodic behavior (vanishing of transient period) raises with the Prandtle number increasing. The reason of this manner is that the inertia force increases with the viscosity force increasing which depends on fluid type.

Obviously, the Prandtle number variations have no effect on the flow field. Whereas, the variation of Prandtle number has significant effect on heat transfer as it is presented in several figures. In **Fig. 31** and **Fig. 32**, it can be observed that the local Nusselt number increases with the increasing of the Prandtle number because of the rate of temperature change with respect to the Y-direction high value. This high rate of change value is clearly shown in **Fig. 35** and **Fig. 36** for linear and sinusoidal temperature variation correspondingly. For the same reason the thermal boundary layer thickness decreases with increasing Prandtle number values as illustrated in **Fig. 33** and **Fig. 34**.

Finally, an attempt was made to study the effect of the non-dimensional period and amplitude variation for the sinusoidal temperature boundary condition at the lower boundary near the flat plate. Results for this attempt are presented in several figures. The effect of the non-dimensional period on the variation of the local Nusselt number at the end of the flat plate is illustrated in **Fig. 37**. From this figure, it is clear that the local Nusselt number increases slightly with the rising of the non-dimensional period increasing. While there is not any difference in the temperature rate of change with respect to Y-direction as it is noticed from **Fig. 38**. Similar figures are sketched in order to demonstrate the effect of the non-dimensional amplitude. The same trends of curves are obtained when sketching these figures in order to express the effect of non-dimensional amplitude variation in **Fig. 39** and **Fig. 40**. From these two figures, it can be observed that the local Nusselt number increases with increasing amplitude and also there is not any significant change in the temperature rate of change with increasing amplitude. The reason of the increasing in local Nusselt number is due to the direct relation with the temperature.

The heat transfer characteristics of the present issue for the linear temperature variation with position and sinusoidal temperature variation with time cases are sketched in the following two figures. These figures include the heat transfer characteristics of previous work [Qahtan 2005] with constant temperature condition for the lower boundary. In **Fig. 41**, it is found that the temperature gradient in Y-direction for the sinusoidal temperature case is identical to that of Qahtan. However, the temperature gradient for the linear temperature case has a little distinction in magnitudes but the same trend of curves. This behavior leads to a similar trend of curves for the local Nusselt number variation for Qahtan's work and sinusoidal temperature case as shown in **Fig. 42**.

CONCLUSIONS

The main focus of this research is to study the development of forced convection thermal boundary layer development in a porous media near a flat plate with variable temperature boundary condition by using the finite difference numerical technique. It may be concluded that the rate of heat transfer increases with the Reynolds number and Prandtle number increasing. In addition this rate increases with the inertia effect and Darcy number decreasing. Furthermore, the same trend of curves is obtained for the two cases of temperature boundary condition; the first case is of linear temperature variation with X-direction and the second is of sinusoidal temperature variation with time. It can be deduced that the time required vanishing the transient behavior of the sinusoidal temperature variation and reach a complete periodic behavior increases with the Prandtle number rising. Finally, the increasing of the non-dimensional period and amplitude of the sinusoidal temperature variation boundary condition case yields an increase in the local

Nusselt number. This increasing in Nusselt number leads to an increase in the rate of heat transfer.

REFERENCES

- Anderson, A. D., Tannehill, C. J., and Pletcher, H. R., " Computational Fluid Mechanics and Heat Transfer", Hemisphere, New York, (1984). (case of three authors)
- Beckerman, C., and Viskanta, R., "Force Convection Boundary Layer Flow and Heat Transfer along Flat Plate Embedded in a Porous Media ", Int. J. Heat Mass Transfer, Vol. 30, (1987). (case of two authors)
- Cheng, W. T., and Lin H. T., "Unsteady Forced Convection Heat Transfer on a Flat Plate Embedded in the Fluid-Saturated Porous Medium with Inertia Effect and Thermal Dispersion", Int. J. Heat Mass Transfer, Vol. 45, (2002). (case of two authors)
- Fletcher, C.A.J., " Computational Techniques for Fluid Dynamics 2", Springer –Verlag Berlin Heidelberg New York, (1987). (case of one authors)
- Huang, P.C., and Vafai, K., "Analysis of Flow and Heat Transfer over an External Boundary Covered with a Porous Substrate ", ASME, J. Heat Transfer, Vol. 116, (1994). (case of two authors)
- Huang, P.C., Yang C. F., Hwang J. J., and Chiu, M. T., "Enhancement of Forced-Convection Cooling of Multiple Heated Blocks in a Channel Using Porous Covers", Int. J. Heat Mass Transfer, Vol. 48, (2005). (case of four authors)
- Poulikakos, D., and Kazmierczak, M., "Forced Convection in a Duct Partially Filled a Porous Material" J. Heat Transfer, Vol. 109, (1987). (case of two authors)
- Qahtan A. F. Al-Abidy, "Forced Convection Thermal Boundary Layer Development in a Porous Media Near a Heated Wall", Thesis, University of Technology, (2005). (case of one author)
- Vadakkan U., "Forced Convection through a Duct Containing a Pin Fin Array", ME608 Semester Project, (2001). (case of one author)
- Vafai, K., and Huang, P.C., "Analysis of Heat Transfer Regulation and Modification Employing Intermittently Emplaced Porous Cavities", Trans. ASME, J. Heat Transfer, Vol. 116, (1994). (case of two authors)
- Vafai, K., and Thiyagaraja, R., "Analysis of Flow and Heat Transfer at The Interface Region of Porous Medium ", Int. J. Heat and Mass Transfer, Vol. 30, (1987). (case of two authors)

NOMENCLATURE

Symbols

a : Non-dimensional amplitude.
AL : Inertial parameter for porous medium.
Cp : Specific heat [$J/kg.K$].
Da : Darcy number.
F : A function used in expressing inertia terms.
H : Height of porous medium [m].
k : Thermal conductivity of the porous media.
K : Permeability of the porous medium [m^2].
L : Plate length [m].
Nu : Nusselt number.
p : Pressure N/m^2 .
P : Non-dimensional pressure.
Pr : Prandtl number.
Re : Reynolds number.
t : Time [s].
t^* : Non-dimensional time.
T : Temperature [^oC].
u : $x-$ Component velocity [m/s].
U : $X-$ Component non-dimensional velocity u/u_∞ .
v : $y-$ Component velocity [m/s].
V : $Y-$ Component non-dimensional velocity v/u_∞ .
V_m : Mean value of X and $Y-$ velocity components.

x : Horizontal coordinates.
X : Non-dimensional horizontal coordinate.
y : Vertical coordinates.
Y : Non-dimensional vertical coordinate.

Greek Symbols

α : Thermal diffusivity [m^2/s].
ε : Porosity.
η : Non-dimensional period.
ψ : Non-dimensional stream function.
ω : Non-dimensional vorticity.
ϑ : Non-dimensional temperature.
σ : Thermal capacity ratio.
ρ : Density [kg/m^3].
μ : Dynamic viscosity of fluid [$N.s/m^2$].

Subscript

∞ : Free stream.
f : Fluid.
p : Fluid inside porous media.
eff : Effective.
w : Wall.
s : Solid.

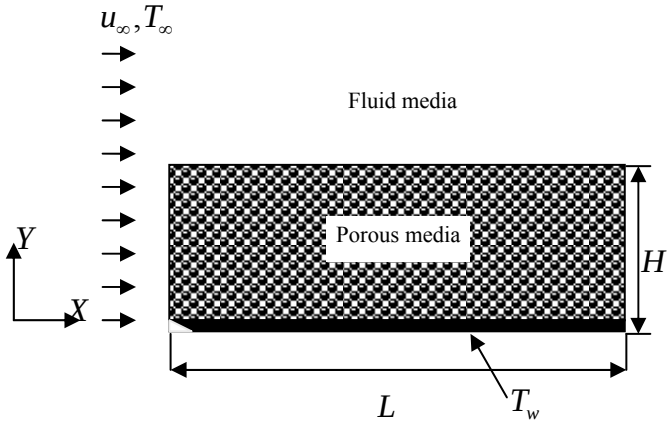

Fig. (1): The Schematic Diagram of the Physical Model.

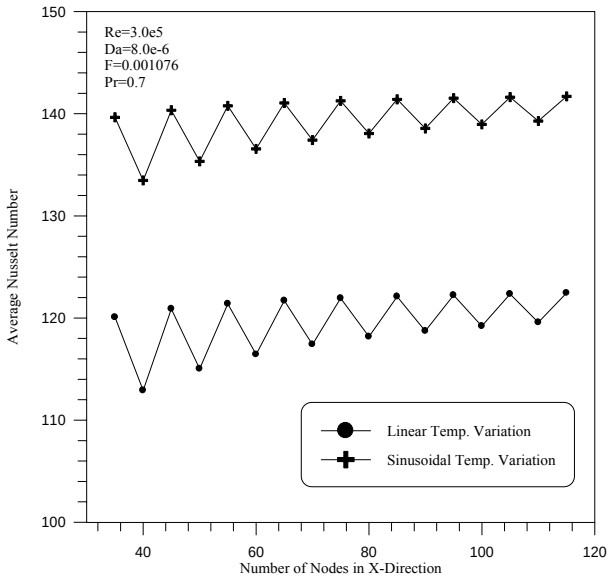

Fig. (2): Average Nusselt Number versus Number of Nodes in X-Direction (Linear and Sinusoidal

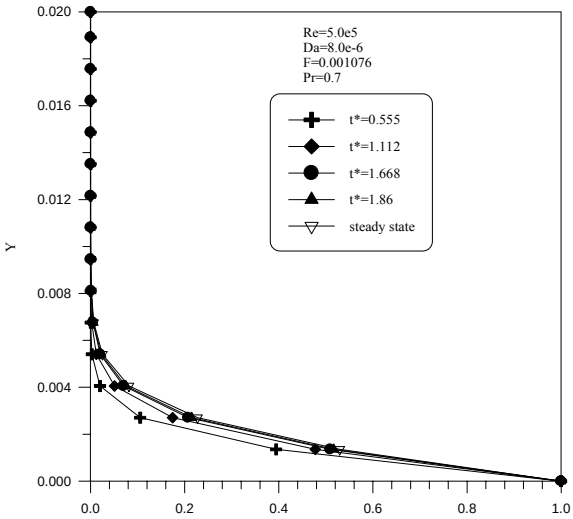

Fig. (3): Propagation of the Non-Dimensional Temperature with Time (Linear).

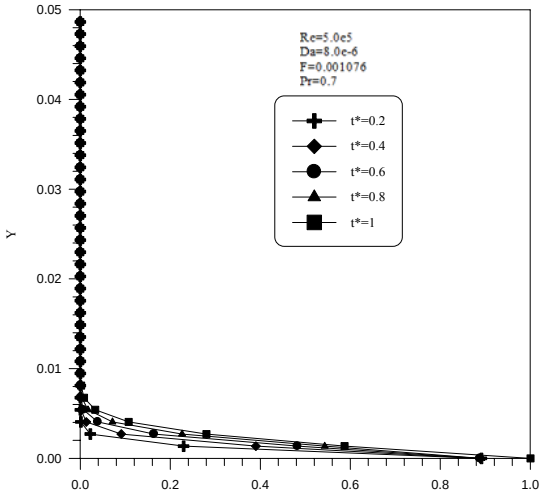

Fig. (4): Propagation of the Non-Dimensional Temperature Time (Sinusoidal).

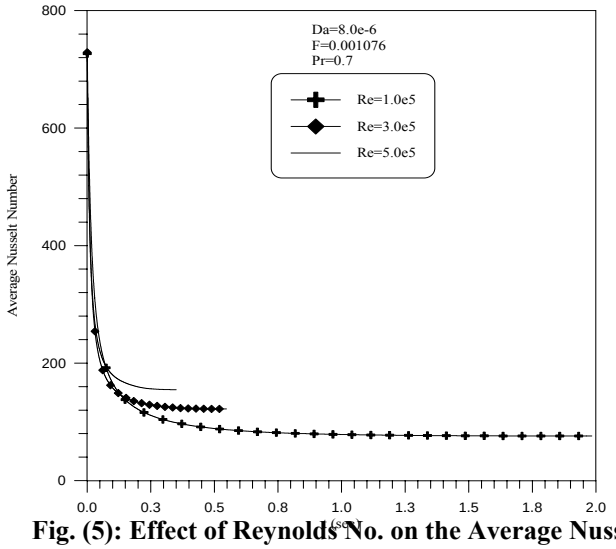

Fig. (5): Effect of Reynolds No. on the Average Nusselt Number Variation with Time (Linear).

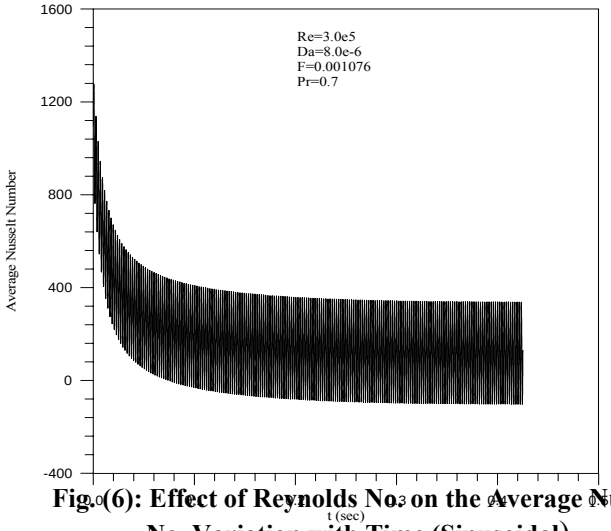

Fig. (6): Effect of Reynolds No. on the Average Nusselt No. Variation with Time (Sinusoidal).

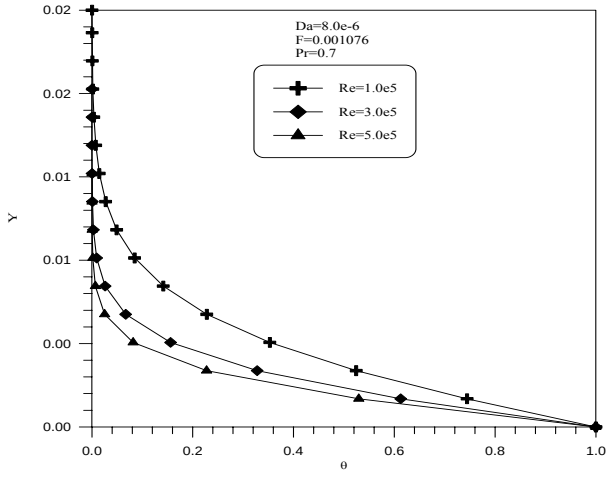

Fig. (7): Effect of Reynolds No. on the Temperature at the Flat Plate End (Linear).

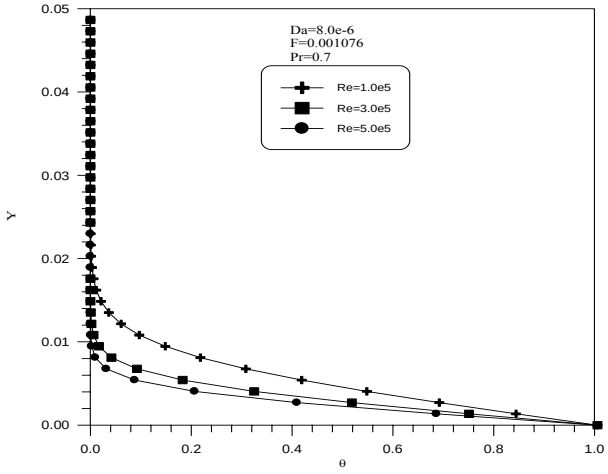

Fig. (8): Effect of Reynolds No. on the Temperature at the End of the Flat Plate (Sinusoidal).

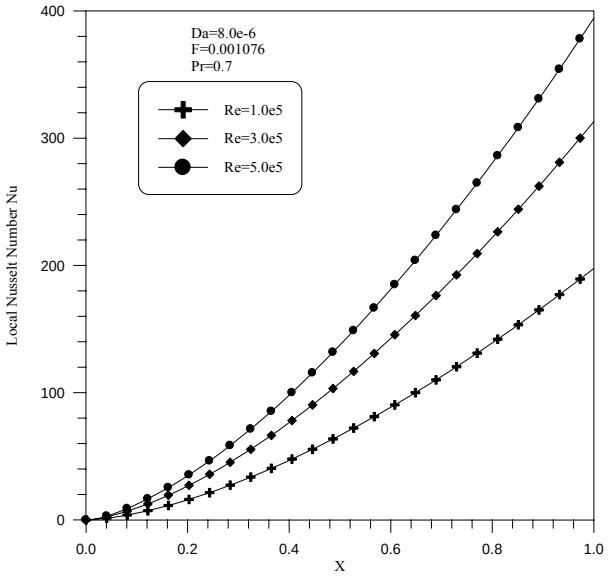

Fig. (9): Effect of the Reynolds Number on the Local Nusselt No. along the Flat Plate (Linear).

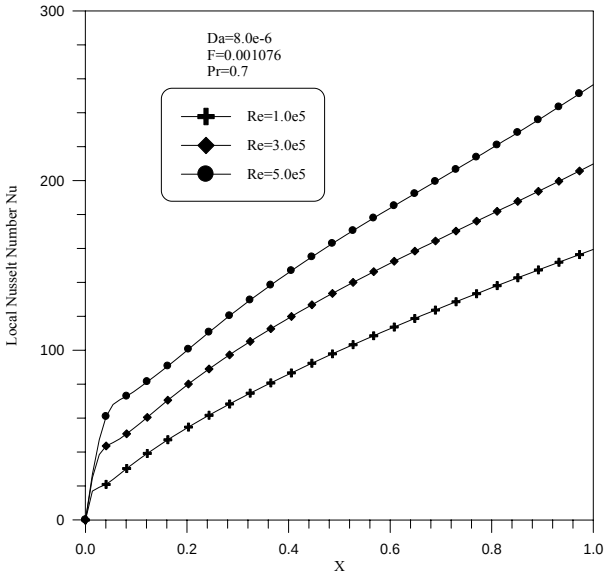

Fig. (10): Effect of the Reynolds Number on the Local Nusselt No. along the Flat Plate (Sinusoidal).

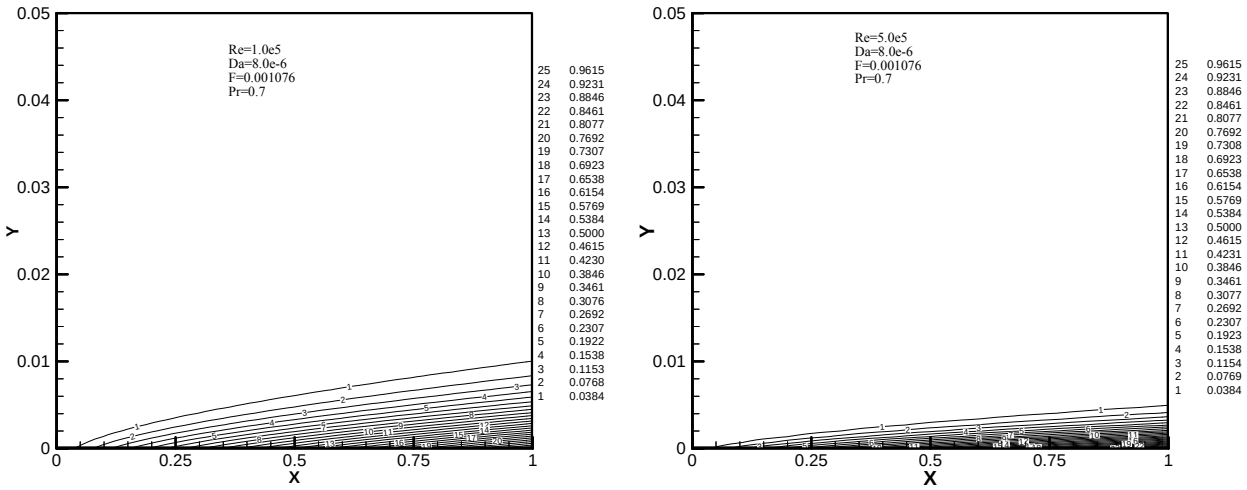

Fig. (11): Distribution of the Non-Dimensional Temp. at Various Reynolds Number (Linear).

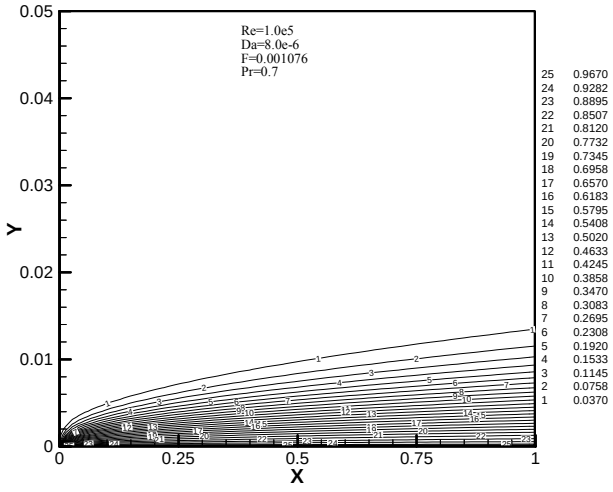

Fig. (12): Distribution of the Non-Dimensional Temp. at Various Reynolds Number (Sinusoidal).

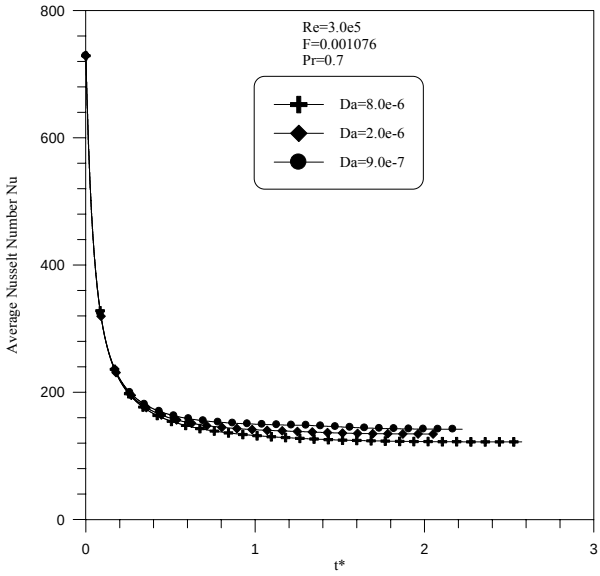

Fig. (13): Effect of Darcy Number on the Average Nusselt Number with Time (Linear).

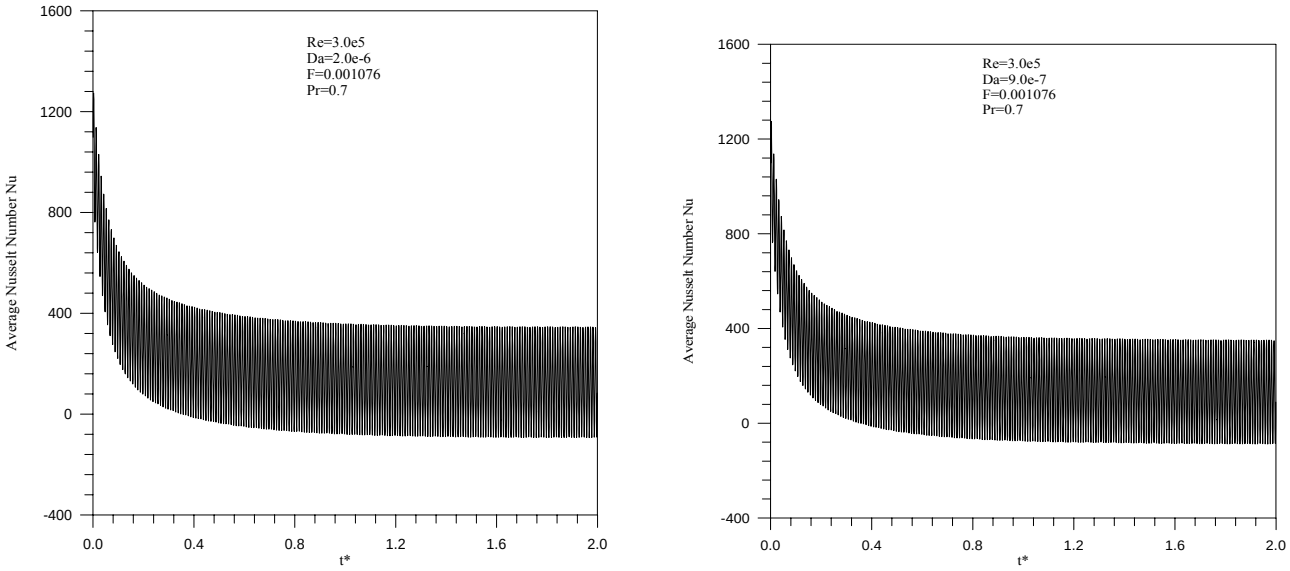

Fig. (14): Effect of Darcy Number on the Average Nusselt Number with Non-Dimensional Time for Specified Reynolds Number (Sinusoidal).

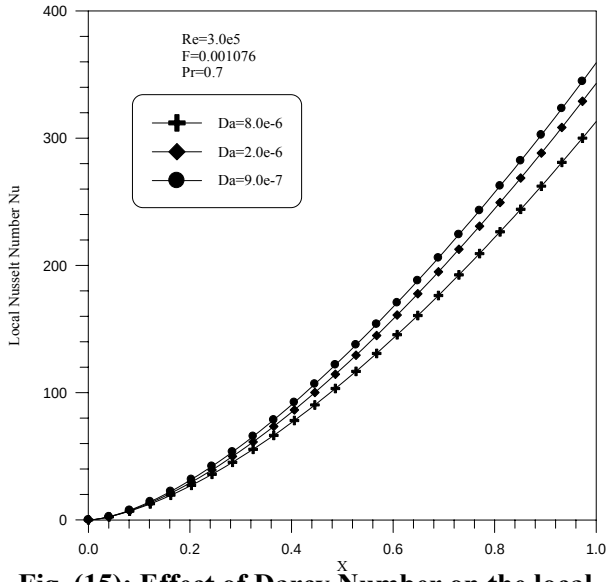

Fig. (15): Effect of Darcy Number on the local Nusselt Number along the Flat Plate (Linear).

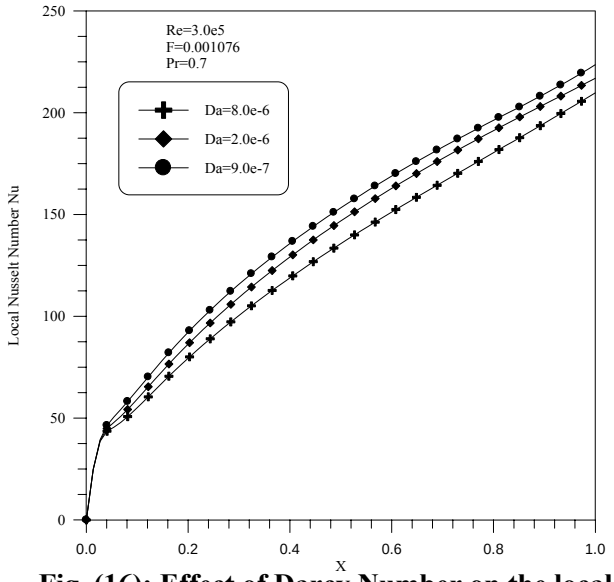

Fig. (16): Effect of Darcy Number on the local Nusselt Number along the Flat Plate (Sinusoidal).

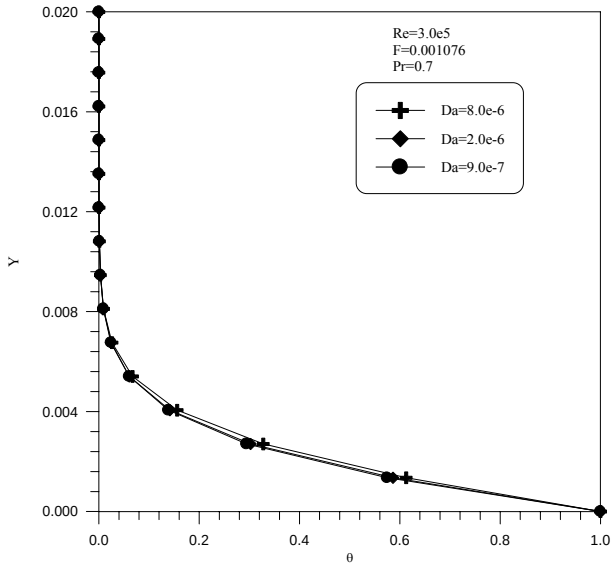

Fig. (17): Effect of Darcy Number on the Non-Dimensional Temp. at the Flat Plate End (Linear).

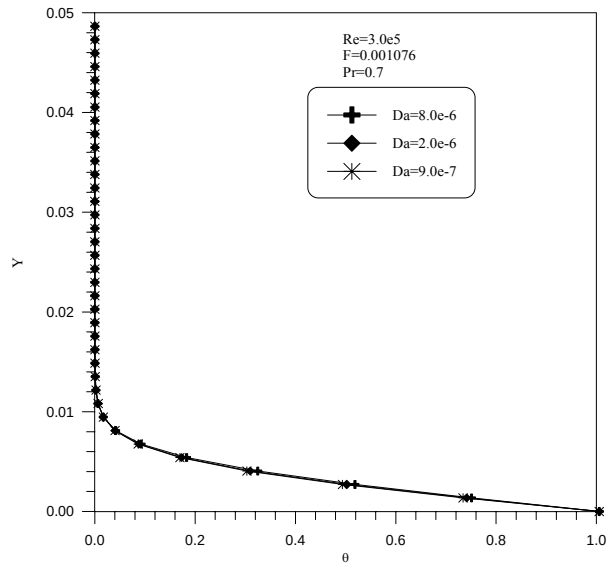

Fig. (18): Effect of Darcy Number on the Non-Dimensional Temp. at the Plate End (Sinusoidal).

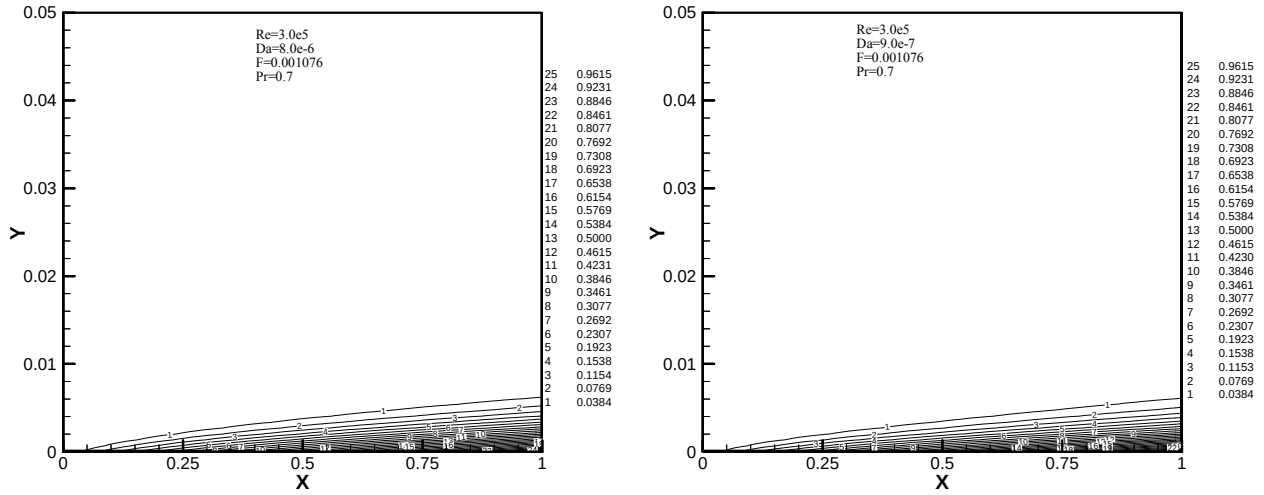

Fig. (19): Distribution of the Non-Dimensional Temp. at Various Darcy Number (Linear)

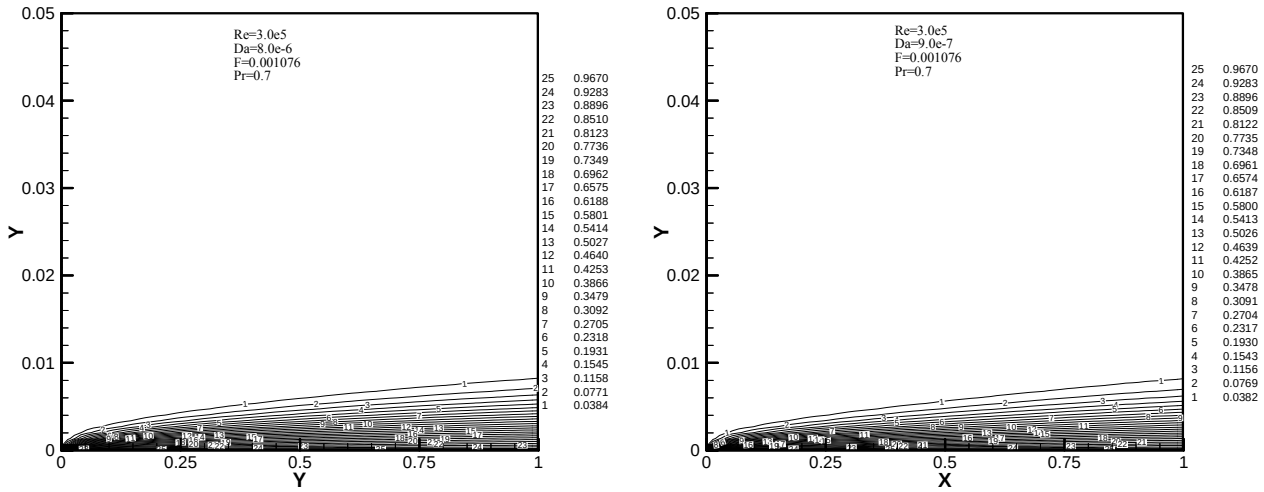

Fig. (20): Distribution of the Non-Dimensional Temp. at Various Darcy Number (Sinusoidal).

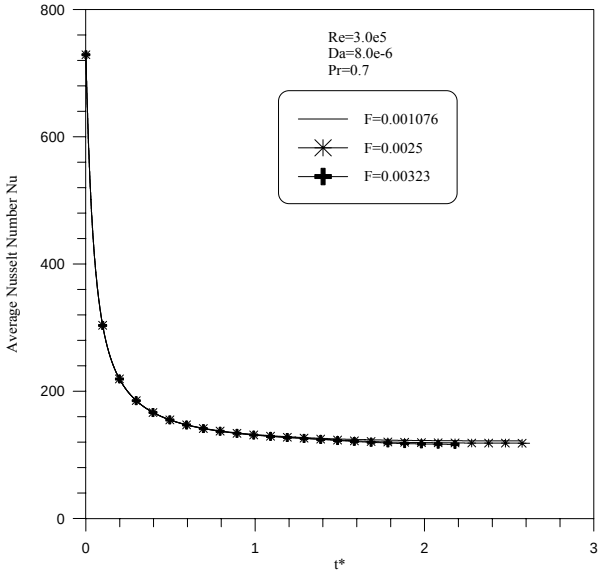

Fig. (21): Effect of Inertia on the Average Nusselt Number with Non-Dimensional Time (Linear).

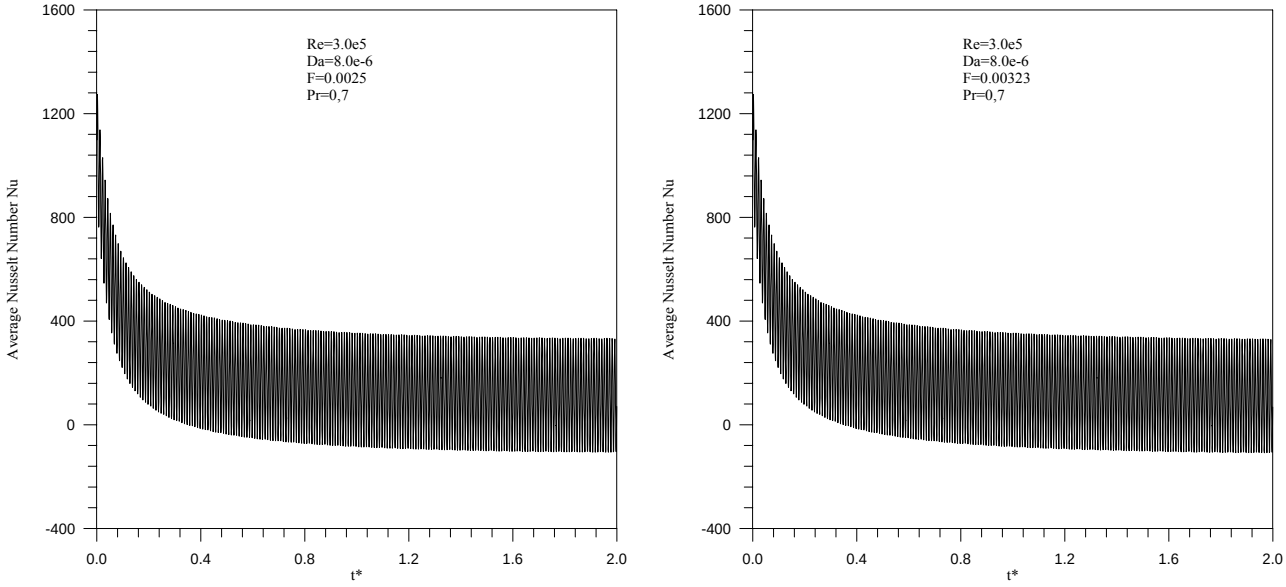

Fig. (22): Effect of Inertia on the Average Nusselt Number with Time (Sinusoidal).

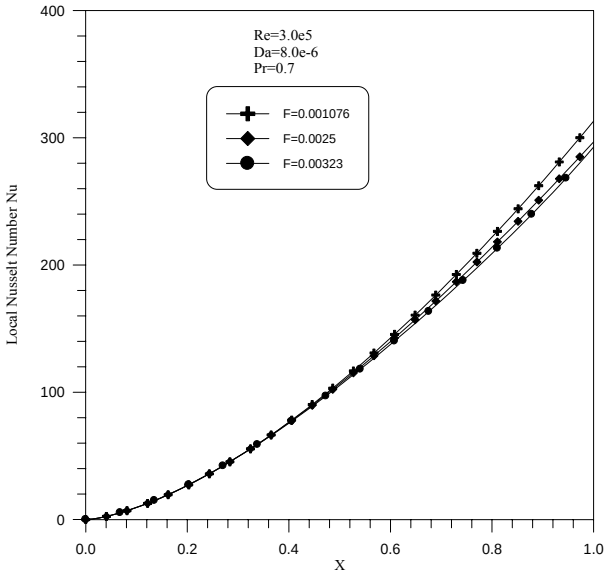

Fig. (23): Effect of Inertia on the local Nusselt Number along the Flat Plate (Linear).

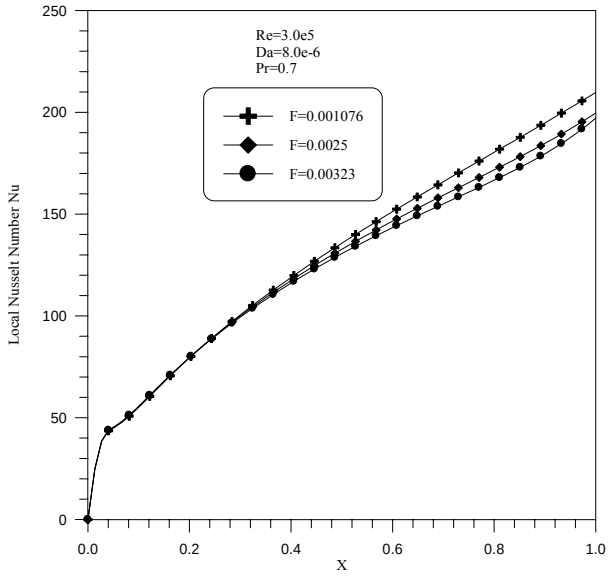

Fig. (24): Effect of Inertia on the local Nusselt Number along the Flat Plate (Sinusoidal).

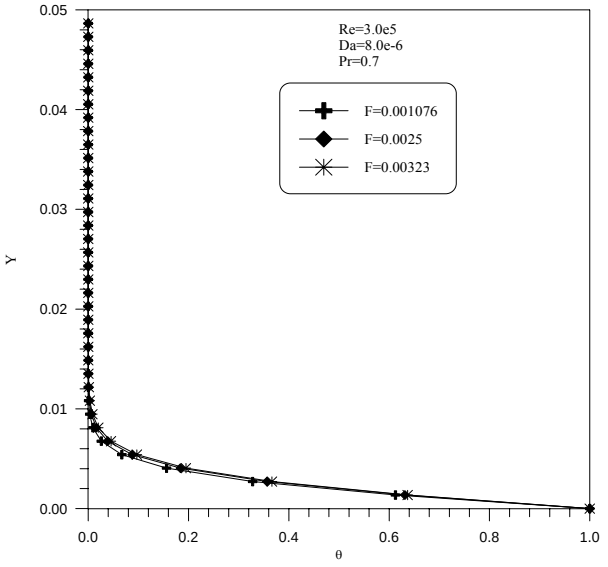

Fig. (25): Effect of Inertia on the Temperature at the Flat Plate End (Linear).

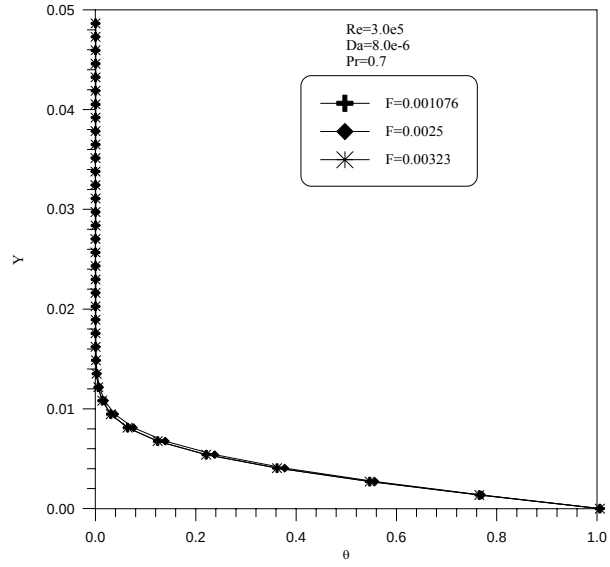

Fig. (26): Effect of Inertia on the Temperature at the End of the Flat Plate (Sinusoidal).

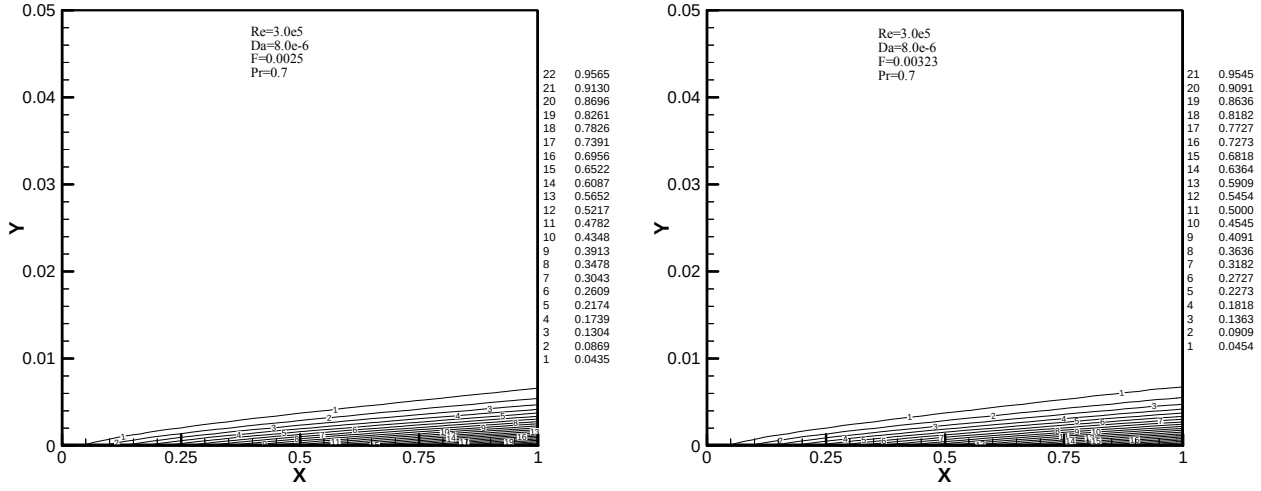

Fig. (27): Effect of Inertia on the Temperature Distribution at Specific Reynolds Number (Linear).

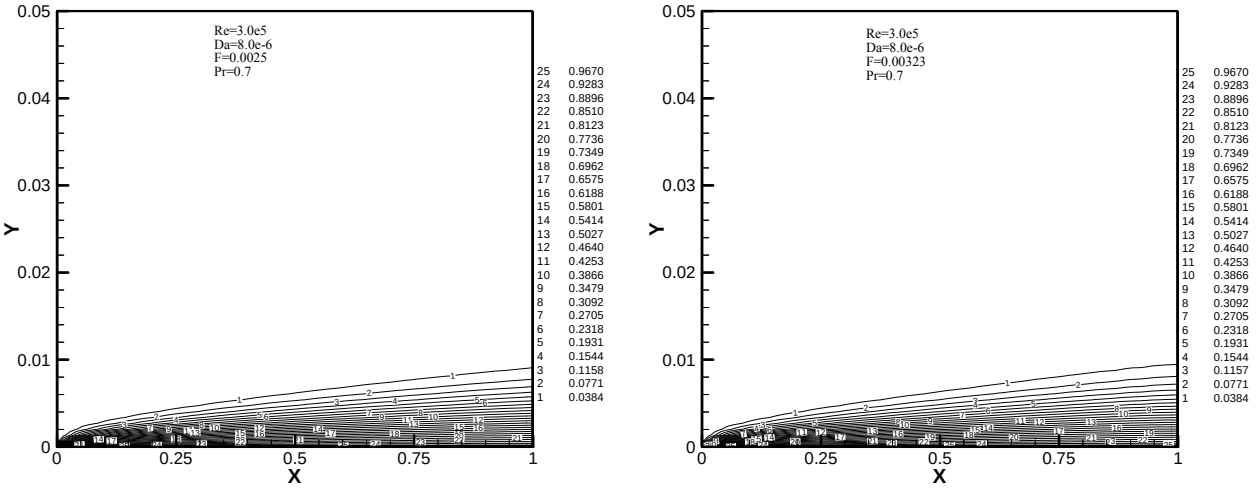

Fig. (28): Effect of Inertia on the Temp. Distribution at Specific Reynolds Number (Sinusoidal).

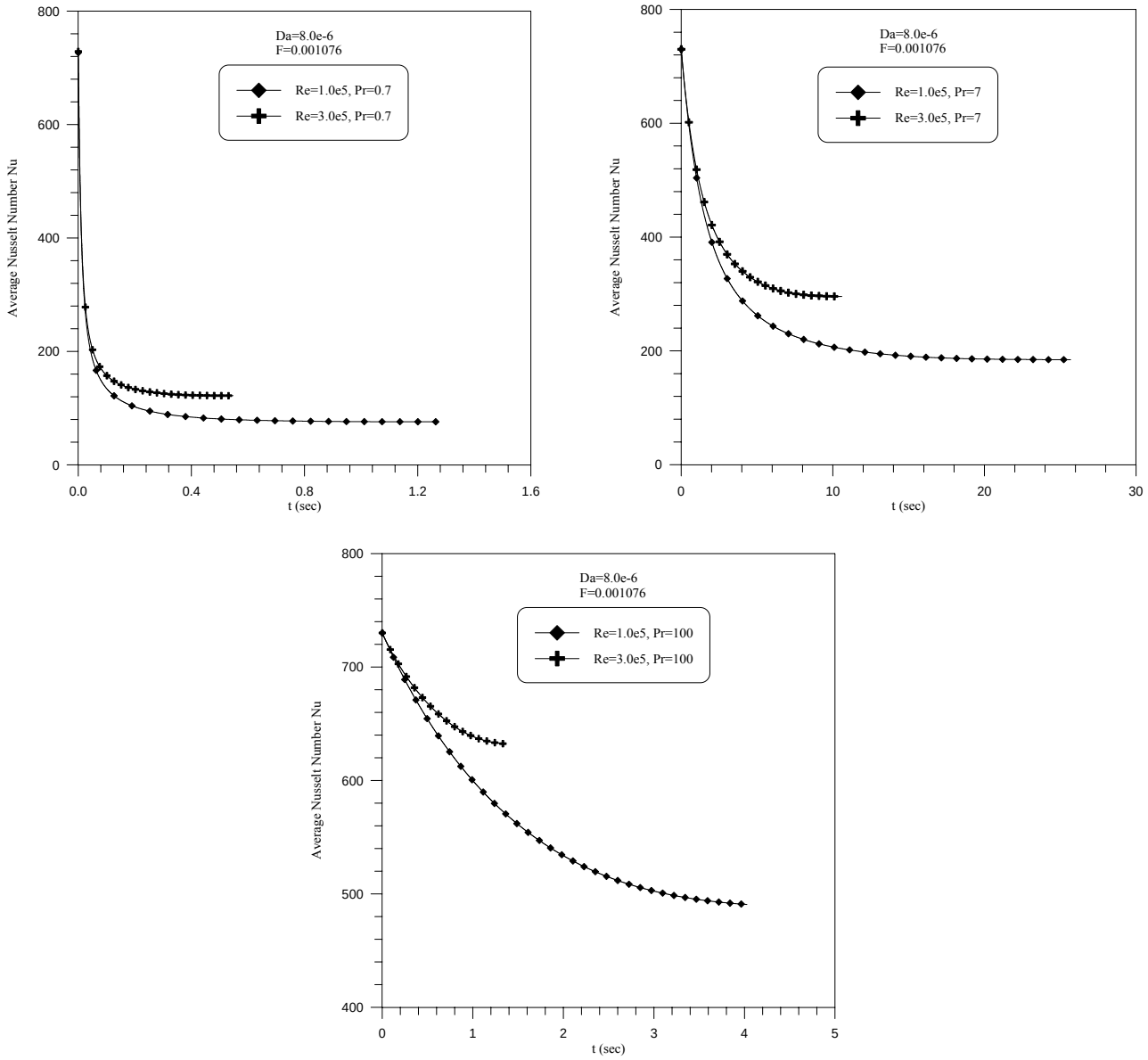

Fig. (29): Effect of Prandtle Number on the Average Nusselt Number Variation with Time at Specific Reynolds Number (Linear).

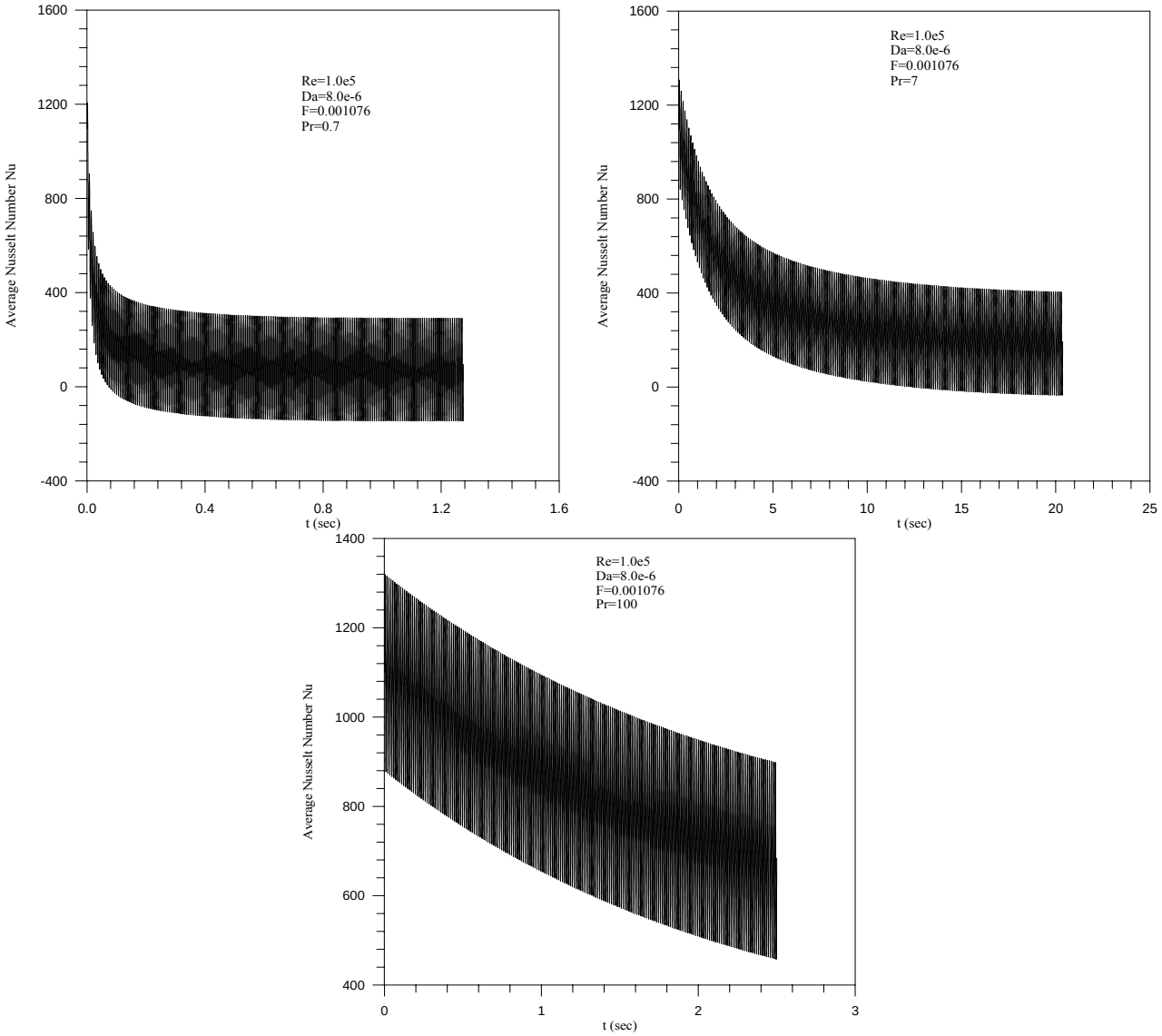

Fig. (30): Effect of Prandtle Number on the Average Nusselt Number Variation with Time at Specific Reynolds Number (Sinusoidal).

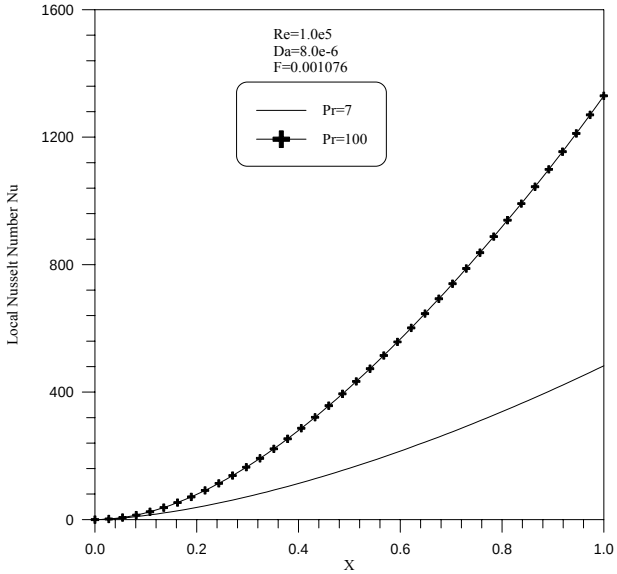

Fig. (31): Effect of Prandtle Number on the Local Nusselt Number Variation with Time (Linear).

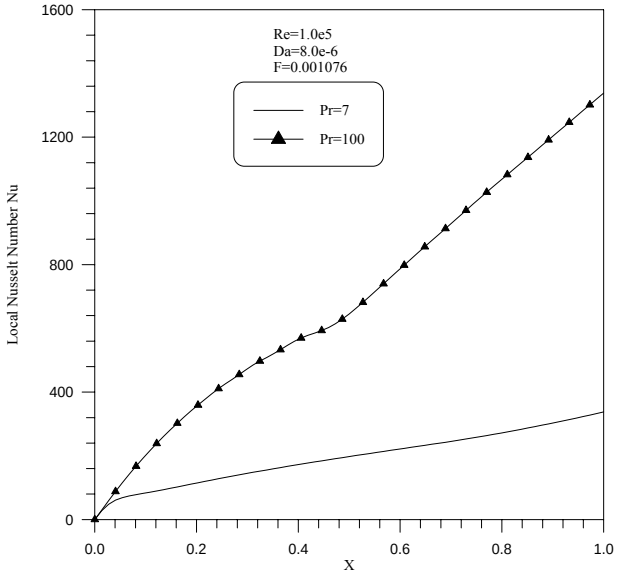

Fig. (32): Effect of Prandtle Number on the Local Nusselt Number Variation with Time (Sinusoidal).

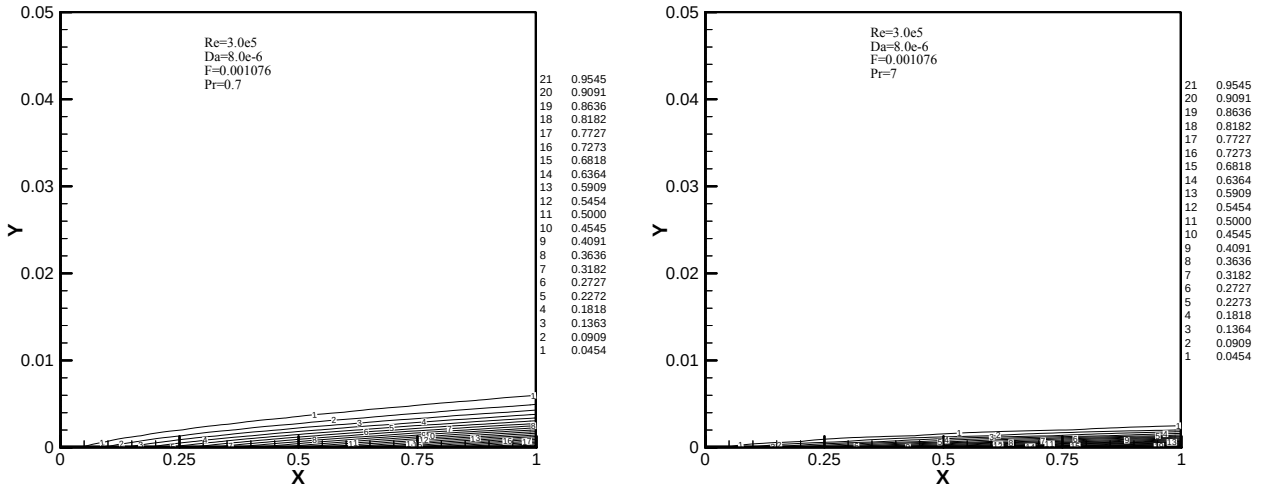

Fig. (33): Effect of Prandtle Number on the Temperature Distribution (Linear).

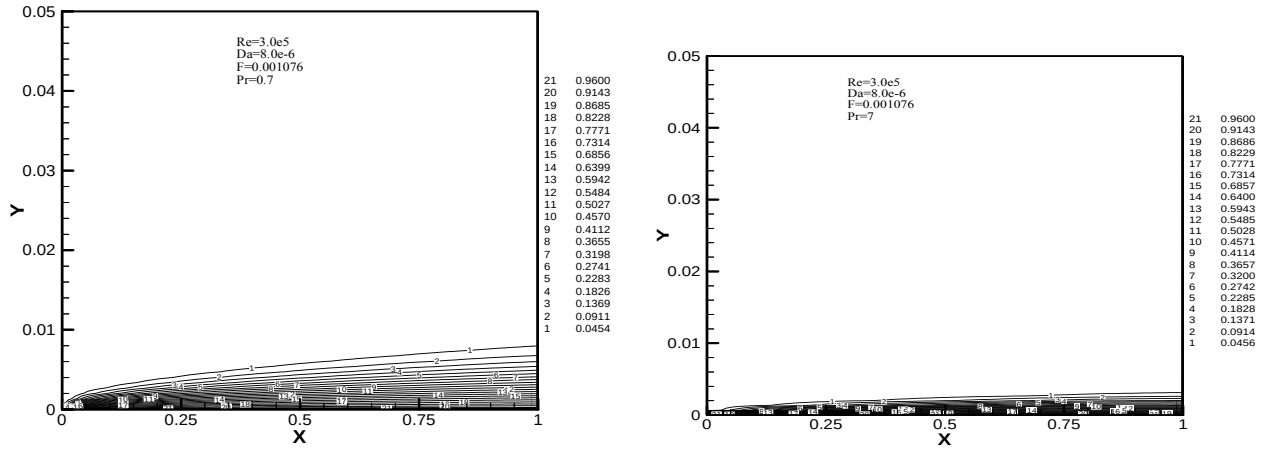

Fig. (34): Effect of Prandtle Number on the Non-Dimensional Temp. Variation (Sinusoidal).

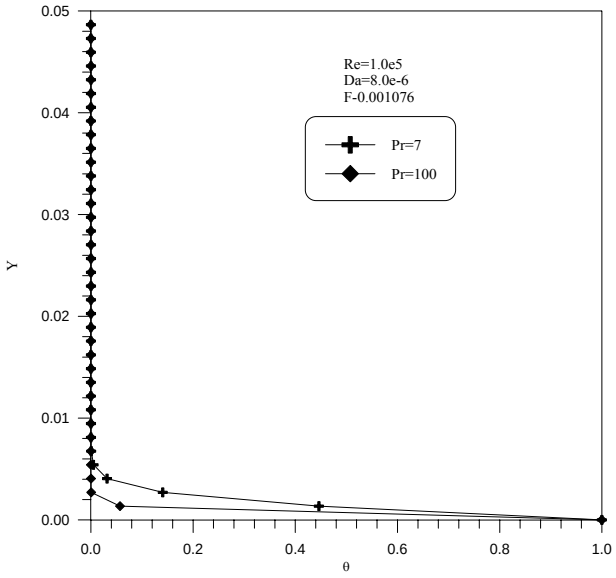

Fig. (35): Effect of Prandtle Number on the Temperature at the Plate End (Linear).

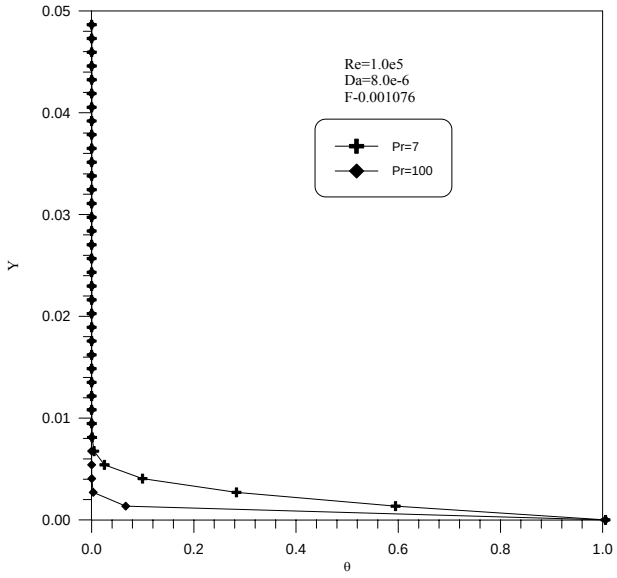

Fig. (36): Effect of Prandtle Number on the Temperature at the Plate End (Sinusoidal).

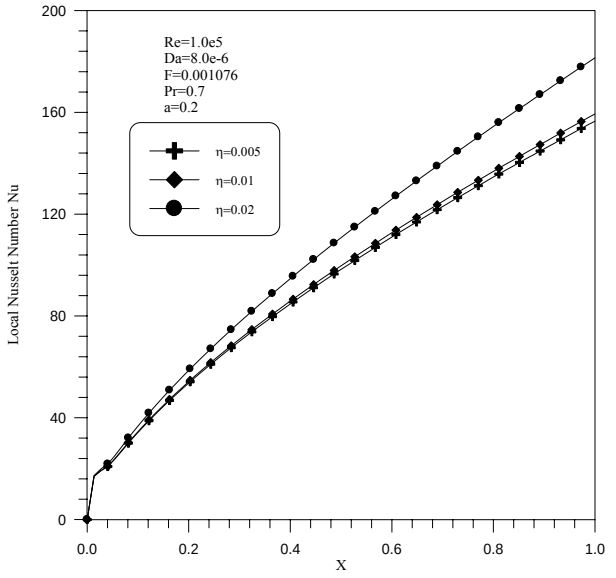

Fig. (37): Effect of Period on the Local Nusselt Number Variation (Sinusoidal).

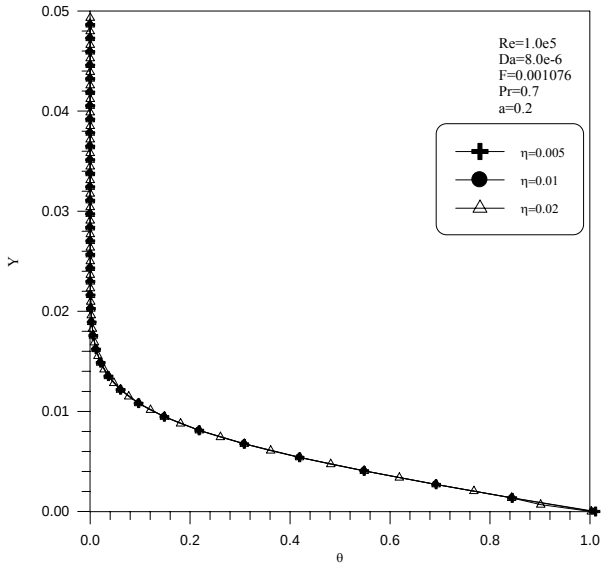

Fig. (38): Effect of Period on the Temperature at the Plate End (Sinusoidal).

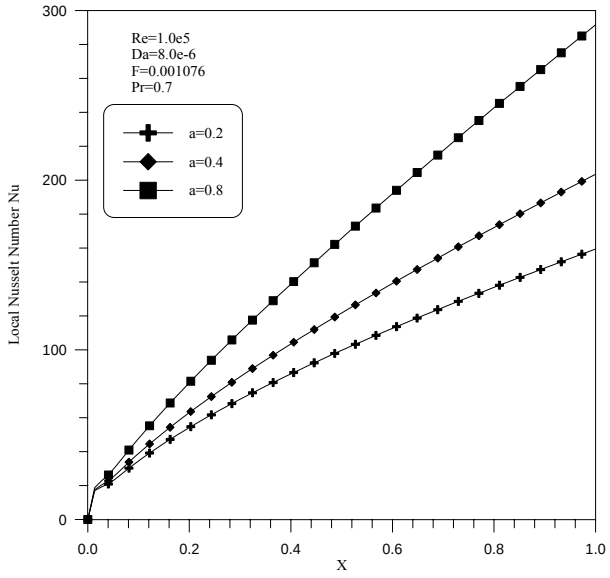

Fig. (39): Effect of Amplitude on the Local Nusselt Number Variation for $\eta = 0.01$ (Sinusoidal).

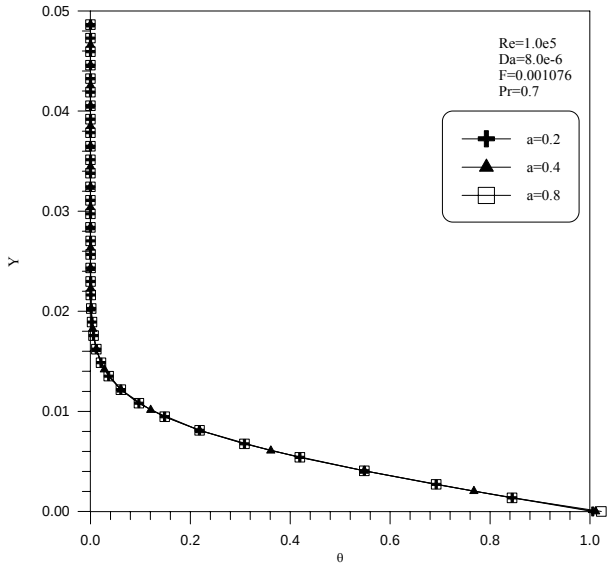

Fig. (40): Effect of Amplitude on the Temperature at the Plate End for $\eta = 0.01$ (Sinusoidal).

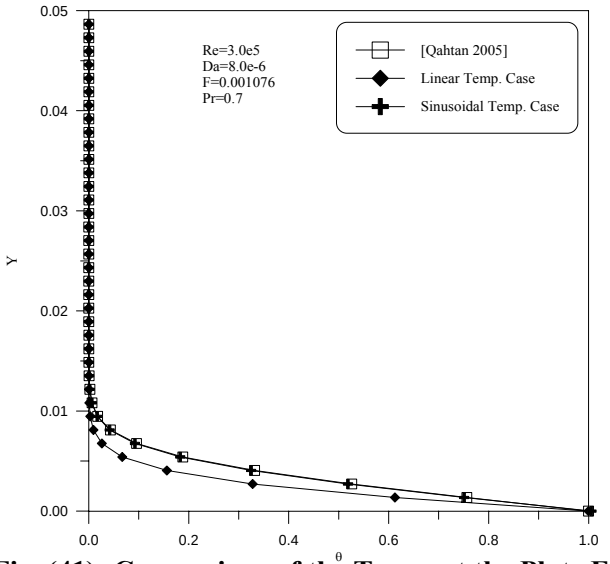

Fig. (41): Comparison of the Temp. at the Plate End for the Two Temp. Cases and Recent Work

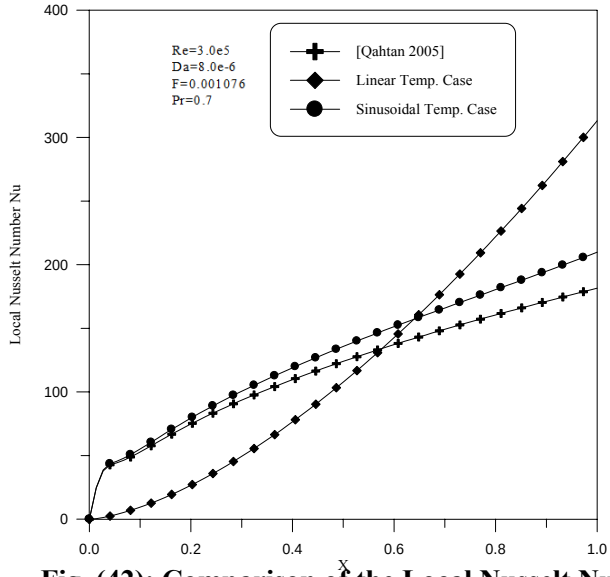

Fig. (42): Comparison of the Local Nusselt Number for the Two Temp. Cases and Recent Work